Transient deformation measurement by double-pulsed-subtraction TV holography and the Fourier transform method

A. Fernández, J. Blanco-García, A. F. Doval, J. Bugarín, B. V. Dorrío, C. López, J. M. Alén, M. Pérez-Amor and J. L. Fernández

Departamento de Física Aplicada. Universidade de Vigo
ETSEIM Lagoas-Marcosende, 9. E36200 Vigo (SPAIN)

Phone: +34 86 812 216
Fax: +34 86 812 201
E-mail: antfdez@uvigo.es

We report the measurement of transient bending waves with double-pulsed-subtraction TV holography. The correlation fringe patterns are automatically, quantitatively analyzed by the application of Fourier methods. A novel optical setup based on an arrangement resembling the Mach-Zehnder interferometer is demonstrated for the generation of carrier fringes. The proposed system is highly immune to environmental disturbances because it imposes no limit to the time separation between laser pulses. The linear phase distribution due to the spatial carrier is removed in the spatial domain by subtracting the phase of the undeformed carrier fringes from the phase of the modulated fringes. Experimental results obtained with an aluminum plate excited by the impact of a piezoelectric translator are presented.

Keywords: Pulsed TV holography, transient deformation measurement, Fourier transform method

1. Introduction

Electronic speckle pattern interferometry (ESPI), or television holography (TVH) as it is also known, is a well-established technique for optical metrology. Over the past two decades, it was successfully used in a wide range of applications, such as deformation measurement, vibration analysis, surface contouring, fluid flow visualization and nondestructive testing.[1,2] Within the field of deformation measurement, the study of the instant response of objects to impact loading is a subject of great interest in engineering, and constitutes one of the most appealing applications of TV holography. Transient deformation analysis involves rapid variations of phase that prevent the use of temporal phase measurement methods[3] because all the information necessary to calculate a phase map from the fringe pattern must be recorded simultaneously. Spatial methods are very well suited for phase demodulation of transient fringe patterns as phase information is available from a single video frame.

Interesting work describing transient deformation measurement has been published in recent years. Pedrini *et al.*[4,5] have experimentally demonstrated the application of the spatial-carrier phase-shifting method to transient analysis with double-pulse-subtraction TV holography, a fringe generation technique formerly proposed by Spooren.[6] They use a standard ESPI setup in which the reference beam is tilted by an angle θ with respect to the optical axis. This angle is chosen so that the phase difference between the object and reference beams changes by a constant amount (usually 90º or 120º) from one pixel to the adjacent one in the tilt direction. Phase is calculated from irradiance values for sets of 3 consecutive pixels using standard phase-shifting algorithms. This method is attractive for industry because of its experimental simplicity together with the low computing time required for the complete analysis of an interferogram. However, it has several drawbacks. It presumes that there is little variation in the irradiance of the interfering waves over any set of 3 consecutive pixels, which is not true for the general case of a diffusely reflecting object. Furthermore, the spatial resolution is limited by the size of speckle, that must be at least 3 pixels wide, and the resulting phase maps are corrupted by speckle noise.

A research group at the University of Luleå, Sweden, has proposed an elegant method for the evaluation of spatial carrier phase-shifted TV holograms[7] and applied it to the measurement of transient bending waves in plates with double-pulsed-subtraction TV holography.[8] The spatial carrier is introduced by setting a small angular offset between the object and reference beams. They record a Fourier spectrum of the fringe pattern by using a properly designed aperture lens that forms the image on the photosensitive surface of the detector. Phase is calculated by inverse Fourier transforming the parts of the spectrum that correspond to the interference between the reference and the object beams. Three different apertures were tested: single slit, double slit and three-hole. The three-hole aperture is advantageous in that the spatial resolution is equal in the horizontal and vertical directions of the image, and the random speckle noise can be reduced by speckle averaging.[8] Furthermore, it makes also possible to measure the in-plane displacement in addition to the out-of-plane normally measured. Unfortunately, the three hole aperture reduces the total area of the aperture, giving rise to a waste of laser energy and a lost of spatial resolution.

An alternative method of transient vibration analysis with pulsed ESPI has been recently proposed.[9-12] Spatial carrier is generated by properly tilting the reference beam between two laser pulses. The main difference with respect to the two methods above is that the spatial carrier is introduced in the correlgrams (correlation fringe patterns) rather than in the specklegrams (speckle interferograms). Two different systems were developed for that aim. In the first one, the key element is a Pockels cell located in the reference beam path, that polarizes the laser light either vertically or horizontally. The output of the Pockels cell is directed to a Michelson arrangement with a polarizer beam splitter. Depending on the polarization of the laser pulse, light passes through either one arm of this arrangement or the other. Carrier fringes appear when one of the mirrors in the Michelson arrangement is slightly tilted.[9,10] In the second of these systems, a galvanometer mounted mirror is incorporated to the reference beam. The galvanometer is used to tilt the reference beam[11,12] in order to produce a linear phase term, and hence carrier fringes, in the correlation fringe pattern. The experimental setup of the second system is much simpler than the first one. However, it imposes a minimum separation between laser pulses, determined by the galvanometer response time, which is several orders of magnitude longer than the response time of the Pockels cell in the first system (500 μs against 15 ns respectively). The aforementioned limit negates the advantages of double-pulsed ESPI, as the system based on the galvanometer is sensitive to external disturbances, thus being unsuitable to operate in industrial environments.

In a recent paper, we have reported the measurement of transient bending waves in plates by single-pulsed-subtraction TV holography and the Fourier transform method.[13] Spatial carrier is introduced in the correlgrams displacing manually between pulses the negative lens that expands the object beam in a standard ESPI setup. This technique was demonstrated in laboratory conditions, although the long time required for the lens displacement (several seconds) is unacceptable for working in noisy environments. Bonding the negative lens to a piezoelectric transducer could significantly reduce the minimum separation between pulses. This solution was adopted by other authors in a double-pulsed-addition ESPI system for harmonic vibration measurement.[14] However, they found that the use of a piezo-mounted lens to generate carrier fringes reduced the immunity of their double-pulsed TVH system to environmental disturbances because the piezoelectric element had a response time of 200 μs.

An improvement of our previous system is presented here. We study the early propagation of transient bending waves induced by mechanical impact in plates by double-pulsed-subtraction TV holography. Phase is evaluated by the Fourier transform method (FTM), a technique originally conceived and demonstrated by Takeda *et al*.[15] We propose a novel optical setup to introduce a spatial carrier in the correlgrams by shifting the object beam between laser pulses. The optical system is experimentally simple and imposes no limit to the time separation between pulses. A complete description of the fringe analysis is presented, as well as experimental results.

2. Theory

2.1. Fringe Formation

The study of transient deformations by double-pulsed-subtraction TVH involves the recording of two specklegrams in separate TV fields,[6] each corresponding to an instantaneous state of dynamic deformation of the object's surface. The first specklegram, which is recorded with the object at rest, can be expressed mathematically as follows[1]

$$i_1(x,y) = i_{obj}(x,y) + i_{ref}(x,y) + 2\left[i_{obj}(x,y)i_{ref}(x,y)\right]^{1/2} cos\,\psi(x,y) \tag{1}$$

where $i_1(x,y)$ is the intensity at a point (x,y) of the speckle pattern, $i_{obj}(x,y)$ and $i_{ref}(x,y)$ are the intensities at (x,y) that correspond to the object and the reference wave fronts, respectively, and $\psi(x,y)$ is the optical phase difference between the two wave fronts, which is random because of the object surface roughness.

The second specklegram, recorded after the object was impact loaded, has the following expression

$$i_2(x,y) = i_{obj}(x,y) + i_{ref}(x,y) + 2\left[i_{obj}(x,y)i_{ref}(x,y)\right]^{1/2} cos\left[\psi(x,y) + 2\pi u_c x + \phi(x,y) + \varphi(x,y)\right] \tag{2}$$

where $\phi(x,y)$ denotes the optical phase difference due to the object surface deformation, $\varphi(x,y)$ represents a phase change due to rigid body motion or any other environmental disturbance between pulses, and $2\pi u_c x$ is the phase of the spatial carrier (see section 3). Time dependence has been omitted in Eqs. (1) and (2) because of the extremely short pulse duration (typically 20 ns), that effectively freezes an instant of the transient deformation.

Provided that the time separation between pulses is short in double-pulsed TV holography (typically 1÷100 μs), the phase term corresponding to rigid body motion can be neglected, $\varphi(x,y) = 0$ in Eq. (2). In that case, subtraction of specklegram $i_1(x,y)$ from $i_2(x,y)$, followed by full wave rectification of the result, yields a high visibility correlation fringe pattern expressed by

$$\left|i_1(x,y) - i_2(x,y)\right| = \left|4\left[i_{obj}(x,y)i_{ref}(x,y)\right]^{1/2} \sin\left[\psi(x,y) + \frac{2\pi u_c x + \phi(x,y)}{2}\right] \sin\frac{2\pi u_c x + \phi(x,y)}{2}\right| \tag{3}$$

2.2. Fringe Analysis

In this section we describe phase extraction from double-pulsed-subtraction TVH correlation fringe patterns by the Fourier transform method (see Refs. 3, 15 and 16 for a more detailed description of the general method). Neglecting the effect of speckle noise in the correlgram, equation (3) can be approximated by the first two terms of its Fourier expansion

$$\left|i_1(x,y) - i_2(x,y)\right| \approx \frac{8}{\pi}\left[i_{obj}(x,y)i_{ref}(x,y)\right]^{1/2} - \frac{16}{3\pi}\left[i_{obj}(x,y)i_{ref}(x,y)\right]^{1/2} cos\left[2\pi u_c x + \phi(x,y)\right] \tag{4}$$

where $\frac{8}{\pi}\left[i_{obj}(x,y)i_{ref}(x,y)\right]^{1/2}$ and $\frac{16}{3\pi}\left[i_{obj}(x,y)i_{ref}(x,y)\right]^{1/2}$ are the terms corresponding to the background and modulated carrier, respectively.

Defining

$$a(x,y)=\frac{8}{\pi}\left[i_{obj}(x,y)i_{ref}(x,y)\right]^{1/2} \tag{5}$$

and

$$c(x,y)=\frac{8}{3\pi}\left[i_{obj}(x,y)i_{ref}(x,y)\right]^{1/2}\exp\left[j\phi(x,y)\right] \tag{6}$$

with $j=\sqrt{-1}$, Fourier transform of equation (4) yields

$$\mathrm{F}\{i_1(x,y)-i_2(x,y)\}\approx A(u,v)-C(u-u_c,v)-C^*(-u-u_c,v) \tag{7}$$

where F represents two-dimensional Fourier transform, capital letters denote Fourier spectra, u and v are horizontal and vertical spatial frequencies respectively, and C^* represents the complex conjugate of C.

Provided that variations of background and phase of interest are slow compared with the spatial carrier frequency u_c, the Fourier spectrum of a double-pulsed-subtraction TVH correlation fringe pattern consists of three separated regions. $A(u,v)$ is centered on the origin of the Fourier plane, and contains the background and low-frequency information. The other two lobes, $C(u\text{-}u_c,v)$ and $C^*(\text{-}u\text{-}u_c,v)$ are offset from the frequency origin by $|u_c|$. By properly masking the Fourier spectrum, $C(u\text{-}u_c,v)$ can be isolated in the frequency domain

$$C(u-u_c,v)=\mathrm{F}\{i_1(x,y)-i_2(x,y)\}W(u,v) \tag{8}$$

being $W(u,v)$ a suitable window in the Fourier plane.

Making use of a well-known Fourier transform property, the inverse two-dimensional FFT of equation (8) can be expressed as

$$\mathrm{F}^{-1}\{C(u-u_c,v)\}=c(x,y)\exp(2\pi j u_c x) \tag{9}$$

and substitution of Eqs. (6) and (8) in Eq. (9) together with argument calculation results in

$$\phi(x,y)+2\pi u_c x=tan^{-1}\left\{\frac{Im\left[\mathrm{F}^{-1}\{\mathrm{F}\{i_1(x,y)-i_2(x,y)\}W(u,v)\}\right]}{Re\left[\mathrm{F}^{-1}\{\mathrm{F}\{i_1(x,y)-i_2(x,y)\}W(u,v)\}\right]}\right\} \tag{10}$$

Expression (10) is the sum of the phase due to the transient deformation and that of the spatial carrier. This phase is indeterminate to a factor of 2π because the arctangent is defined over a range from $-\pi$ to $+\pi$. In order to isolate the phase of interest, the phase map given by equation (10) is unwrapped and carrier phase is removed in the spatial domain (see section 5). Finally, the out-of-plane component of the transient deformation is calculated by

$$z(x,y)=\frac{\lambda}{4\pi}\phi(x,y) \tag{11}$$

where λ is the wavelength of the laser light.

3. Experimental Setup and Spatial Carrier Generation

The experimental setup is shown in Fig. 1. The light source is a twin-cavity, diode-seeded Nd:YAG pulsed laser. Each cavity produces 12 mJ in 20 ns pulses at a rate of 25 Hz. Their infrared outputs are recombined by means of a beam combiner BC1 and frequency doubled in order to make alignment and signal detection easier and safer. The resulting green laser radiation (532 nm) is split into two beams: reference beam (≈10% of the energy), which is launched to a monomode optical fiber for convenience, and object beam, which is expanded though a negative lens NL2 to illuminate the object. If the mirror M3 is given a small tilt (exaggerated in the diagram), light from cavity 1 goes through a different path than light from cavity 2. In that case, light from cavity 1 is directed by mirrors M4, M5 and M6 to the negative lens NL1, that is mounted on a X-Y translation stage TS allowing displacement of the lens perpendicular to its optical axis. Once expanded by NL1 and NL2 respectively, the object beams are recombined at BC2 and illuminate the object. Mirrors M4, M5 and M6 together with beam combiner BC2 form an arrangement resembling the Mach-Zehnder interferometer. Both reference and object beams are added coherently by means of a beam combiner BC3 and imaged onto the photosensitive surface of an interline-transfer CCD camera. Optical paths are equalized to maximize contrast. Moreover, the polarization of the reference beam is adjusted by means of a polarization controller PC to fit the polarization of the object beam. The optimal speckle size can be achieved by adjusting the objective camera aperture. The interferometer is sensitive to the out-of-plane component of the object surface deformation.

In order to introduce a spatial carrier in the double-pulsed-subtraction TVH correlation fringe patterns, the negative lens NL1 is displaced across a plane perpendicular to its optical axis by means of the X-Y translation stage TS. For the particular case of an horizontal lens displacement, it results in a linear phase term $2\pi u_c x$ in Eqs. (2) and (3). If the test object is not excited between lasers pulses, $\phi(x,y) = 0$ in Eqs. (2) and (3), the correlgram shows a set of equispaced parallel vertical fringes, whose spatial frequency u_c is proportional to the displacement of NL1. In the general case of $\phi(x,y) \neq 0$, carrier fringes appear modulated by the transient deformation of the object surface.

Besides the optical components, the system includes a piezoelectric translator to excite transient bending waves, an electronic synchronization system,[17,18] and a computer-based image processor. The synchronization circuit extracts the vertical synchronism pulses from the video signal. These pulses trigger a high precision programmable delay generator that provides laser firing and piezo translator excitation signals thus synchronized with image acquisition. The delay generator is programmed to fire the first laser pulse at the end of the even field, and the second one at the beginning of the odd field of the same video frame. The delay between the piezo translator triggering and the second laser pulse can be readily measured by means of a rapid photodetector and a memory oscilloscope and it is also adjusted by properly programming the delay generator.

The operation of the double-pulsed-subtraction TVH system is as follows. The laser continuously emits twin-pulses at a rate of 25 Hz, conveniently timed with respect to the video signal. When the operator gives the order to start, the test object is impacted by the piezo translator between the laser pulses as stated before and the resulting video frame is digitized and stored as a 512×512×8 bits image in a frame grabber board. The even lines of such image contain the irradiance values recorded by the CCD during the first laser pulse. They form the reference specklegram, expressed by Eq. (1). The specklegram corresponding to the transient deformation, Eq. (2), is contained in the odd lines. Next, a frame processor subtracts even lines from the adjacent odd ones and rectifies the result, yielding a high visibility correlation fringe pattern, Eq. (3), that presents a set of equispaced vertical carrier fringes modulated by the transient deformation. Time required for the frame processor to accomplish the analysis of such a single correlgram using the Fourier transform method, Eqs. (4) through (11), is approximately 1 minute.

4. Results

The system described in section 3 was used to measure transient bending waves in metallic plates. Provided that the induced transient deformation is statistically repetitive, a sequence of phase maps representing the temporal evolution of the transient waves can be formed by repeating the experiment with different values of the delay between the mechanical impact and the second laser pulse, as shown in Fig. 2. The specimen used in our experiment is an aluminum alloy plate (300 mm × 120 mm × 3.5 mm) clamped along its left and right edges. An area of approximately 85 mm (*X* direction) × 65 mm (*Y* direction) was measured. Time separation between laser pulses was set to 50 μs. Exact delay between the piezo translator excitation signal and the firing of the second laser pulse is placed beneath each column. This delay is the sum of the amplifier and the piezo translator response times, that are unknown, plus the actual delay between the mechanical impact and the second laser pulse. These response times are estimated to be ≈10 μs, by comparison with previous experiments in which the delay between mechanical impact and second laser pulse was accurately measured.[16] The spatial carrier is set to 11 vertical fringes across the image by displacing 0.20 mm the negative lens NL1 in Fig. 1 (focal length –25 mm) along the horizontal direction normal to its optical axis. Fig. 2(a)-(c) shows correlation fringe patterns recorded at three different propagation instants, that consist of those 11 vertical carrier fringes modulated by the transient deformation. Their corresponding phase maps, deformation plus carrier, and three-dimensional plots of mechanical deformation after phase unwrapping and carrier removal are shown in Figs. 2(d)-(f) and 2(g)-(i), respectively.

5. Discussion

The system we developed has two main advantages for its industrial application. On the one hand, it is experimentally simple. On the other hand, it is highly immune to environmental disturbances as it imposes no limit to the minimum time separation between laser pulses. Obviously, this is only completely true when the double-pulsed TVH system is operated in the addition mode, because in the subtraction mode the separation between pulses have to be equal to or greater than the transfer period of the camera (≈1 μs in an interline-transfer CCD).[6] The inherent immunity to noise of our system is strongly affected by the method employed for carrier removal. Several methods have been proposed to remove the phase term due to the carrier in either the spatial or the spatial frequency domains.[16] The one we used measures the carrier phase by recording a correlgram prior to the deformation, $\phi(x,y) = 0$ in Eq. (3), and then subtracts it from Eq. (10).[19] This method reduces dramatically the immunity to environmental disturbances, because it is necessary to record two correlgrams, one apart 40 ms from the other. Nevertheless, we chose it because it is the most accurate and works satisfactorily in laboratory conditions. Carrier removal by least-squares-fitting[20] involves larger phase errors. However, this method is best suited when the immunity to external disturbances is critical, as long as just one correlgram is used. The choice between one carrier removal method or another depends on the application.

Ideally, carrier frequency should be high, in order to separate the three main regions of the Fourier spectrum of the correlgram (section 2.2). In practice, there is an upper limit to the carrier frequency imposed by the sampling theorem, as the CCD has a finite number of pixels. In our experiments, we empirically selected the carrier frequency as high as possible while ensuring that no phase discontinuities appeared, following the approach of Takatsuji *et al*.[21]

Phase retrieval by the FTM is strongly affected by the characteristics of the filtering window $W(u,v)$, Eq. (8). Regarding to the window size, large masks are desirable in order to preserve as much information as possible. However, if the mask size grows up excessively, the phase maps are corrupted by discontinuities and distortion, so a compromise must be found. In addition, several weighting functions[22] and shapes[23] have been proposed in the literature for the filtering window. We found that best results are obtained when a *circ* function is used. The frequency coordinates of the center of this circular domain are set to the same values than the peak of the sidelobe of the Fourier spectrum, and its diameter to the maximum value that yields a phase map without discontinuities.

6. Conclusions

We have reported a new method for the measurement of transient deformation by double-pulsed-subtraction television holography. Optical interference phase was calculated directly from the correlgrams using the Fourier transform method. We have designed an original optical setup for the generation of carrier fringes, based on an arrangement resembling the Mach-Zehnder interferometer. Experimental results with a metallic plate excited by impact have been shown to illustrate the performance of this approach. Our system is well suited for industrial applications because of its experimental simplicity and its inherent immunity to external disturbances. Finally, a compromise must be found between accuracy and immunity to disturbances in order to select the best suited method for carrier removal.

This work was funded by the following institutions: Xunta de Galicia (XUGA 32101B95), Comisión Interministerial de Ciencia y Tecnología (TAP95-0805-E) and Universidade de Vigo.

References

1. R. Jones and C. Wykes, *Holographic and Speckle Interferometry*, 2nd ed. (Cambridge University Press, Cambridge, 1989).
2. J. C. Davies and C. H. Buckberry, "Television holography and its applications", in *Optical Methods in Engineering Metrology*, D. C. Williams Ed., (Chapman & Hall, 1993), pp. 275-338.
3 M. Kujawinska, "Spatial phase measurement methods", in *Interferogram Analysis*, D. W. Robinson and G. T. Reid Ed., (IOP Publishing Ltd., 1993), pp.141-193.
4 G. Pedrini and H. J. Tiziani, "Double-pulse electronic speckle interferometry for vibration analysis", Applied Optics **33,** 7857-7863 (1994).
5 G. Pedrini, B. Pfister, and H. J. Tiziani, "Double pulse-electronic speckle interferometry", Journal of Modern Optics **40,** 89-96 (1993).
6 R. Spooren, "Double-pulse subtraction TV holography", Optical Engineering **31,** 1000-1007 (1992).
7 H. O. Saldner, N.-E. Molin, and K. A. Stetson, "Fourier-transform evaluation of phase data in spatially phase-biased TV holograms", Applied Optics **35,** 332-336 (1996).
8 S. Schedin and P. Gren, "Phase evaluation and speckle averaging in pulsed television holography", Applied Optics **36,** 3941-3947 (1997).
9 A. Dávila, D. Kerr, and G. H. Kaufmann, "Fast electro-optical system for pulsed ESPI carrier fringe generation", Optics Communications **123,** 457-464 (1996).
10 J. N. Petzing, A. Dávila, D. Kerr, and J. R. Tyrer, "Transient vibration analysis using pulsed carrier speckle interferometry", in *Proceedings of the Applied Optics Division Conference* (IOP Publishing Ltd., Bristol, 1996), pp. 268-273.

11 J. N. Petzing, D. I. Farrant, G. H. Kaufmann, D. Kerr, J. R. Tyrer, and B. F. Oreb, "The development of pulsed electronic speckle pattern interferometer design for transient vibration analysis", Private communication.

12 D. I. Farrant, G. H. Kaufmann, J. N. Petzing, J. R. Tyrer, B. F. Oreb, and D. Kerr, "Transient deformation measurement using dual-pulse addition ESPI", presented to the *Annual Meeting of the International Society for Optical Engineering*, San Diego, Ca, USA, Optical Science, Engineering and Instrumentation, Conference 3173A, 27 July - 1 August 1997.

13 A. Fernández, A. F. Doval, J. Bugarín, B. V. Dorrío, C. López, J. M. Alén, J. Blanco-García, M. Pérez-Amor, and J. L. Fernández, "Transient bending waves analysis by Fourier evaluation of single pulsed TV-holography fringe paterns", presented to the *European Symposium on Lasers and Optics in Manufacturing*, Munich, FRG, Conference on Optical Inspection and Micromeasurements II, Proc. SPIE 3098, 16-20 June 1997.

14 A. J. Moore and C. Pérez-López, "Double-pulsed addition ESPI for harmmonic vibration and transient deformation measurements", in *Proceedings of the Applied Optics Division Conference* (IOP Publishing Ltd., Bristol, 1996), pp. 228-238.

15 M. Takeda, H. Ina, and S. Kobayashi, "Fourier-transform method of fringe-pattern analysis for computer-based topography and interferometry", Journal of the Optical Society of America **72,** 156-160 (1981).

16 R. W. T. Preater and R. Swain, "Fourier transform fringe analysis of electronic speckle pattern interferometry fringes from high-speed rotating components", Optical Engineering **33,** 1271-1279 (1994).

17 J. Blanco-García, A. F. Doval, A. Fernández, B. V. Dorrío, C. López, R. Soto, J. M. Alén, J. L. Fernández, and M. Pérez-Amor, "Crack detection by TV-holography: continuous and pulsed techniques", in *Proceedings of the Second Iberoamerican Meeting on Optics*, Daniel Malacara, Sofía E. Acosta, Ramón Rodríguez Vera, Zacarías Malacara, Arquímedes Morales, Editors, Proc. SPIE 2730, 101-105 (1996).

18 A. Fernández, A. J. Moore, C. Pérez-López, A. F. Doval, and J. Blanco-García, "Study of transient deformations with pulsed TV holography: application to crack detection", Applied Optics **36,** 2058-2065 (1997).

19 J. M. Huntley and J. E. Field, "High resolution moire photography: application to dinamic stress analysis", Optical Engineering **28,** 926-933 (1989).

20 J. Gu and F. Chen, "Fast Fourier transform, iteration, and least-squares-fit demodulation image processing for analysis of single-carrier fringe pattern", Journal of the Optical Society of America A **12,** 2159-2164 (1995).

21 T. Takatsuji, B. F. Oreb, D. I. Farrant, and J. R. Tyrer, "Simultaneous measurement of three orthogonal components of displacement by electronic speckle-pattern interferometry and the Fourier transform method", Applied Optics **36,** 1438-1445 (1997).

22 D. R. Burton and M. J. Lalor, "Managing some of the problems of Fourier fringe analysis", Proc. SPIE 1163, 149-160 (1989).

23 D. Kerr, F. Mendoza, and J. R. Tyrer, "Manipulation of the Fourier components of speckle fringe patterns as part of an interferometric analysis process", Journal of Modern Optics **36,** 195-203 (1989).

Figure captions

Figure 1: Diagram of the experimental setup used to generate carrier fringes in double-pulsed-subtraction TV holography. M1-M6, mirrors; BC1-BC3, beam combiners; BS, beam splitter; L, positive lens; NL1 and NL2, negative lenses; ZL, zoom lens; FO, fiber optic; PC, polarization controller; TS, translation stage; CCD, charge-coupled-device camera.

Figure 2: Propagation of impact induced bending waves in a metal plate. (a)-(c) Double-pulsed-subtraction TV holography correlation fringe patterns. (d)-(f) Corresponding phase maps, deformation plus carrier. (g)-(i) Three-dimensional plots of the out-of-plane component of the transient deformation.

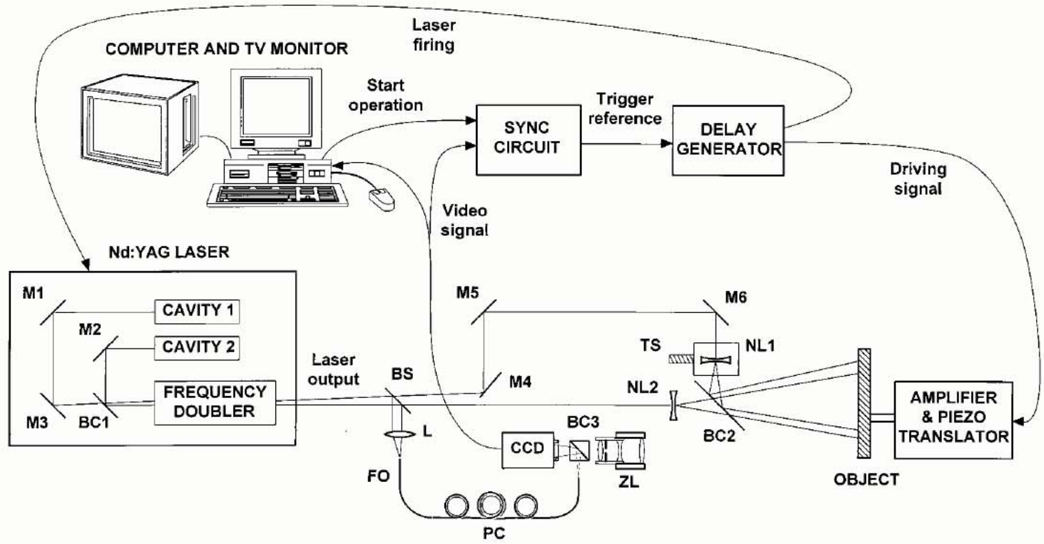

Fig. 1. Diagram of the experimental setup used to generate carrier fringes in double-pulsed-subtraction TV holography: M1–M6, mirrors; BC1–BC3, beam combiners; BS, beam splitter; L, positive lens; NL1, NL2, negative lenses; ZL, zoom lens; FO, fiber optic; PC, polarization controller; TS, translation stage; CCD, charge-coupled-device camera.

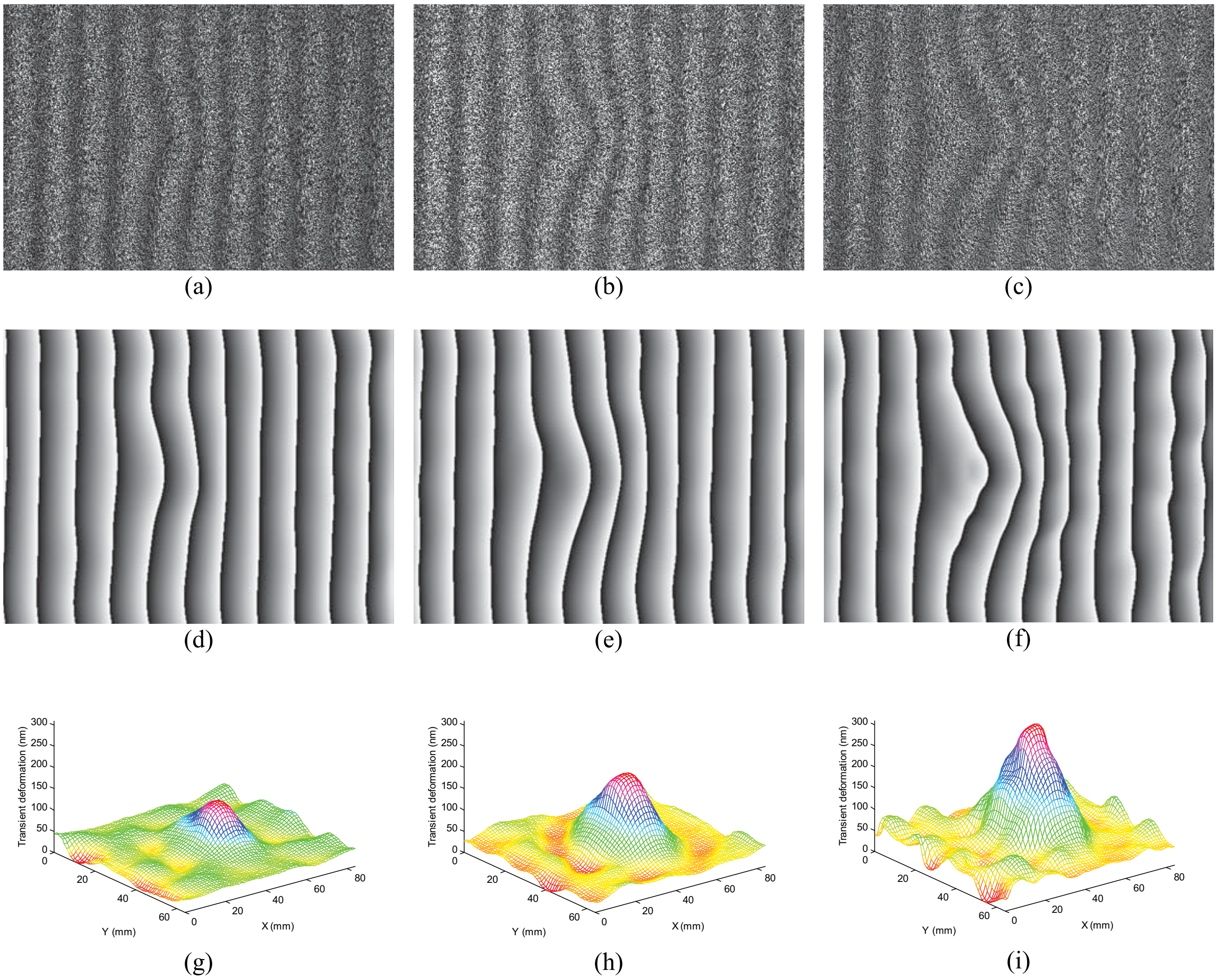

Figure 2
A. Fernández
Applied Optics

NOTE: Please, reduce to two colums width

Propagation of impact induced bending waves in a metal plate. (a)-(c) Double-pulsed-subtraction TV holography correlation fringe patterns. (d)-(f) Corresponding phase maps, deformation plus carrier. (g)-(i) Three-dimensional plots of the out-of-plane component of the transient deformation. Delays between piezo translator driving signal and second laser pulse are 27 μs (left column), 32 μs (central column) and 37 μs (right column).